

Mechanisms of negative cloud radiative feedback of stratocumulus and stratus in JMA-GSM SCM

Hideaki Kawai

Meteorological Research Institute, Japan Meteorological Agency

(e-mail: h-kawai@mri-jma.go.jp)

1. Introduction

In order to understand the mechanism of cloud radiative feedback of marine boundary layer clouds in climate models, a model intercomparison case CGILS (CFMIP-GCSS Intercomparison of Large-Eddy and Single-Column Models) was designed by Minghua Zhang. In the intercomparison case, three different regimes of marine low-level clouds are simulated: shallow cumulus (location: S6), stratocumulus (S11), and stratus (S12). The control climate forcing and the future climate forcing with sea surface temperature increased by 2 K are given for the simulation.

The Single Column Model (SCM) version of the operational global model of the JMA (Japan Meteorological Agency), GSM (Global Spectral Model), was used for the simulation. The results of two versions of this SCM are

shown: one adopts an operational parameterization of stratocumulus (Sc) (Version 1, V1), and the other uses a test version of the Sc parameterization (Version 2, V2). The details of these versions are described by Kawai (2012) (see section 4 of this issue).

2. Negative cloud radiative feedback

The right-hand panel of Fig. 1 reveals that both versions of the JMA-GSM SCM show negative cloud radiative feedback for all cloud regimes (S6: shallow cumulus, S11: stratocumulus, and S12: stratus).

The left-hand panel shows that the liquid water path (LWP) increases for all cloud regimes, using either V1 or V2. The cloud cover is 100% for both the control and future climate forcing, at either S11 or S12, for either V1 or V2 (not shown). Therefore, the negative cloud radiative feedback is a consequence of the increase of LWP for S11 and S12. It is also worth mentioning that the magnitude of the change in cloud feedback is not proportional to the change of LWP: a larger change of LWP at S6 and a smaller change of LWP at S12 bring a comparable change in cloud radiative forcing (CRF). This is because LWP itself is larger at S6, and smaller at S12, and the relationship between LWP and albedo is nonlinear.

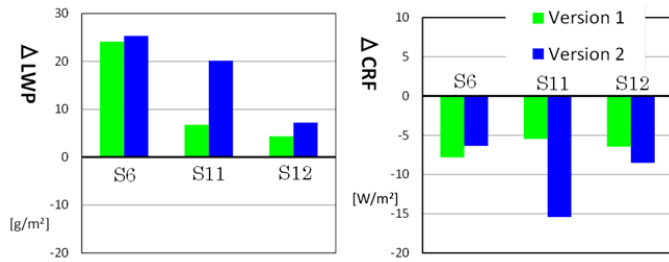


Fig. 1: Changes of liquid water path (left) and cloud radiative forcing (right) between the control climate and future climate forcing. Results are shown for S6, S11, and S12 using Sc scheme Version 1 and Version 2.

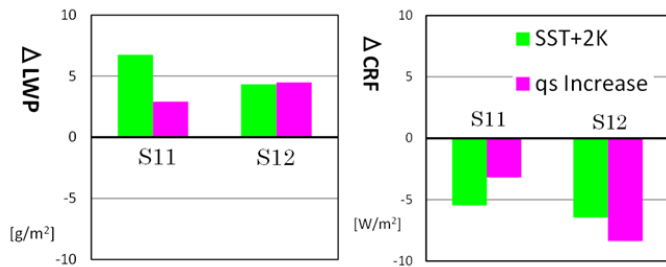


Fig. 2: Changes of liquid water path (left) and cloud radiative forcing (right) between the control climate and future climate forcing (light green), and between using the default parameterization and one with a modified calculation of in-cloud CWC. Results are shown for S11 and S12 using Sc scheme Version 1.

3. Mechanism of increase of LWP

To understand the mechanism of the increase of LWP due to the future climate forcing, simple numerical experiments are performed for each version of the Sc scheme, because the mechanisms could be different for the two parameterizations.

3.1. Mechanism in Sc scheme Version 1

In Sc scheme V1, in-cloud cloud water content (CWC) is determined by the following equation (Kawai 2012):

$$q_{cld} = \beta \cdot q_{sat}$$

As a simple test, the right-hand side of the equation is multiplied by 1.13 using the control climate forcing. This test is performed because when the temperature is increased by 2 K, the saturation specific humidity is increased by about 13%.

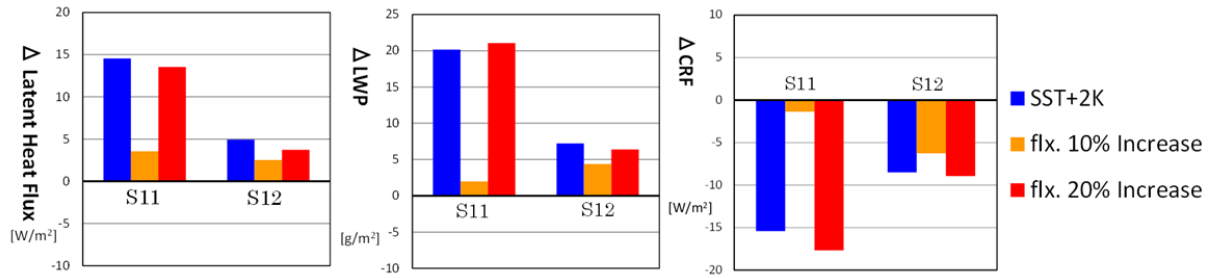


Fig. 3: Change of latent heat flux (left), liquid water path (middle) and cloud radiative forcing (right) between the control climate and future climate (blue), and between the default parameterization and that in which the calculated latent heat flux in the surface flux parameterization is increased by 10% (orange) or 20% (red). Results are for S11 and S12 using Sc scheme Version 2.

Fig. 2 shows that when the factor is increased in the simulation of control climate forcing, the changes of LWP and CRF are comparable to those with future climate forcing, although these changes are not quite identical quantitatively. This result implies that the increase of saturation specific humidity in the future climate contributes to the negative CRF feedback in this scheme. The same mechanism may also generate negative CRF feedback in those models where the same equation is used to determine in-cloud CWC (e.g., diagnostic cloud cover schemes based on relative humidity).

3.2. Mechanism in Sc scheme Version 2

In the case of Sc scheme V2, CWC is determined by a balance of many physical processes. However, the influence of the change of mixing at the cloud top can be ignored in this scheme because the mixing is set to zero (Kawai 2012). In this case, the balance “in the model” can be simplified as follows. There is positive feedback on CWC between

radiative cooling at the cloud top and water vapor transport by turbulence. These two processes can create a balance with the conversion process of CWC to precipitation, because there is a negative feedback on CWC between the former two processes and the conversion process. Based on this concept, a simple test of increasing the latent heat flux is performed. For this purpose, when latent heat flux is calculated in the model by the following equation:

$$Q_E = \rho L C_h |U_1| (q_s - q_1),$$

the flux is multiplied by 1.1 or 1.2 for the control climate forcing simulation.

Figure 3 shows that when the latent heat flux is increased by 10%, the changes of latent heat flux, LWP and CRF are smaller than the changes with future climate forcing. However, it is also clear that those changes are comparable to the change with future climate forcing when the flux is increased by 20%. This result implies that the increase of latent heat flux in the future climate can be, at least partly, a cause of the increase of LWP and hence, negative cloud radiative feedback. It is worth noting that at S11, the changes are much larger for the case of a 20% increase in latent heat flux than for a 10% increase. This large change is caused by a change of vertical structure of the cloud layer. The cloud layer is lifted by one model vertical level at S11 with future climate forcing, as shown in Fig. 4. This discrete lift also occurs in the simulation with a 20% increase of latent heat flux, which destabilizes the sub-cloud boundary layer and results in a step-like transition in the balance among latent heat flux, LWP and CRF.

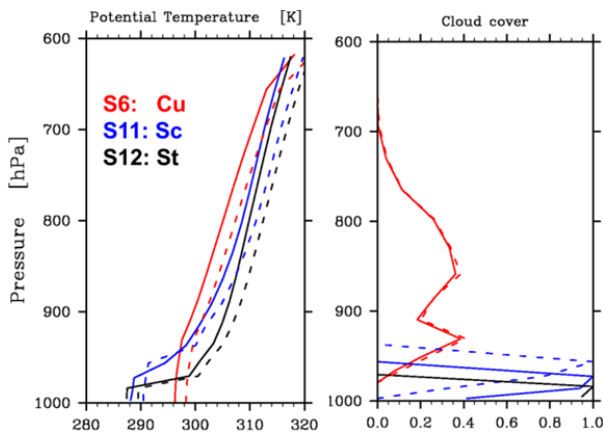


Fig. 4: Vertical profiles of potential temperature (left) and cloud cover (right) for S6, S11, and S12. Solid lines correspond to control climate forcing and dashed lines future climate forcing.

References

Kawai, H., 2012: Results of ASTEX and Composite model intercomparison cases using two versions of JMA-GSM SCM. *CAS/JSC WGNE Research Activities in Atmospheric and Oceanic Modelling/WMO*, **42**, section 4.